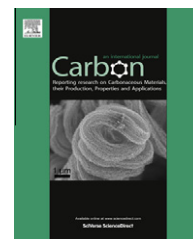


Available at www.sciencedirect.com

SciVerse ScienceDirect

journal homepage: www.elsevier.com/locate/carbon

Towards high purity graphene/single-walled carbon nanotube hybrids with improved electrochemical capacitive performance

Meng-Qiang Zhao, Qiang Zhang^{*}, Jia-Qi Huang, Gui-Li Tian, Tian-Chi Chen, Wei-Zhong Qian, Fei Wei

Beijing Key Laboratory of Green Chemical Reaction Engineering and Technology, Department of Chemical Engineering, Tsinghua University, Beijing 100084, China

ARTICLE INFO

Article history:

Received 10 September 2012

Accepted 24 November 2012

Available online 5 December 2012

ABSTRACT

CoMgAl layered double hydroxides were prepared as catalysts for the *in situ* synchronous growth of graphene and single-walled carbon nanotubes (SWCNTs) from methane by chemical vapor deposition. The as-calcined CoMgAl layered double oxide (LDO) flakes served as the template for the deposition of graphene, and Co nanoparticles (NPs) embedded on the LDOs catalyzed the growth of SWCNTs. After the removal of CoMgAl LDO flakes, graphene (G)/SWCNT/Co₃O₄ hybrids with SWCNTs directly grown on the surface of graphene and 27.3 wt.% Co₃O₄ NPs encapsulated in graphene layers were available. Further removal of the Co₃O₄ NPs by a CO₂-oxidation assistant purification method induced the formation of G/SWCNT hybrids with a high carbon purity of 98.4 wt.% and a high specific surface area of 807.0 m²/g. The G/SWCNT/Co₃O₄ hybrids exhibited good electrochemical performance for pseudo-capacitors due to their high Co₃O₄ concentration and the high electrical conductivity of SWCNTs and graphene. In another aspect, the G/SWCNT hybrids can be used as excellent electrode materials for double-layer capacitors. A high capacity of 98.5 F/g_{electrode} was obtained at a scan rate of 10 mV/s, 78.2% of which was retained even when the scan rate increased to 500 mV/s.

© 2012 Elsevier Ltd. All rights reserved.

1. Introduction

The integration of graphene and carbon nanotubes (CNTs) into a hybrid material is quite a promising way to enhance the dispersion of graphene and CNTs, inherit the virtues of both graphene and CNTs, fabricate an efficient and effective electronic and thermal conductive network, and explore advanced carbon materials [1]. Numerous efforts have been devoted on the fabrication of the graphene/CNT (G/CNT) hybrids, in which the post-organization routes are one of the most initially explored methods. The preparation of highly conductive graphene oxide (GO)/CNT hybrid films

had been firstly reported by Cai et al. through a simple mixing method with the assistance of ultrasonic treatment [2]. G/CNT or GO/CNT hybrids with other structures were also successfully fabricated through the similar liquid phase reaction routes [3] and hydrothermal process [4]. Besides, Bon et al. reported the fabrication of G/CNT hybrid films by electrophoretic deposition [5]. Layer-by-layer (LbL) self-assembly, which is one of the mostly used and effective methods for the fabrication of hybrid materials with different kinds of nanomaterials, has also been explored for the fabrication of G/CNT hybrids. The G/CNT hybrid films were successfully manufactured through LbL assembly of positively charged CNTs and

^{*} Corresponding author: Fax: +86 10 6277 2051.

E-mail address: zhang-qiang@mails.tsinghua.edu.cn (Q. Zhang).

0008-6223/\$ - see front matter © 2012 Elsevier Ltd. All rights reserved.

<http://dx.doi.org/10.1016/j.carbon.2012.11.055>

negatively charged reduced GO nanosheets [6,7]. Hybridization of GO and CNTs was also successfully achieved at the liquid/air interface [8]. The post-organization methods for the fabrication of G/CNT hybrids are effective and scalable. However, the construction of effective connection especially for covalent C–C bonding between graphene and CNTs is extremely complex. Besides, the post-organization methods are also not efficient for the fabrication of G/CNT hybrids based on single-layered graphene and single-walled CNTs (SWCNTs), which are difficult to be well dispersed during the pre-dispersion processes.

Recently, fabrication of G/CNT hybrids through chemical vapor deposition (CVD) is more attractive due to its ability to provide the possibility for the covalent C–C bonding between graphene and CNTs and prepare G/CNT hybrids with various kinds of structures [9–12]. We firstly reported the direct growth of CNTs on the surface of cobalt nanoparticles (NPs) coated GO to fabricate the three-dimensional G/CNT sandwich [13]. A family of G/CNT hybrids with hierarchical structures have also been fabricated through the CVD routes [9,14–17], and some of them were with the assistance of Al_2O_3 [16] and SiO_2 [17] barriers to maintain highly active metal catalyst for CNT growth. The direct growth of CNTs on GO and reduced GO is simple and effective to obtain G/CNT hybrids with strong graphene–CNT bonding and anticipated nanostructures. However, the as-grown CNTs are usually multi-walled CNTs (MWCNTs) and with poor graphitization due to the high dissolubility of catalyst NPs in GO or reduced GO [18]. Besides, the high defect density of GO or reduced GO also limits the quality of graphene in the as-fabricated G/CNT hybrids, and thus hinders their performance. In order to improve the quality of graphene in the G/CNT hybrids, *in situ* growth of G/CNT hybrids on Cu foil coated with Fe catalyst layers was explored [10,19]. However, the as-grown CNTs were still MWCNTs due to the poor stability of the catalyst NPs on metal surface. This results in the low specific surface area (SSA) of the as-fabricated G/CNT hybrids, and hinders their performance in the area where a high SSA is required, such as double-layer supercapacitors. Compared with MWCNTs, the SWCNTs are with much larger surface area and lower defect density. Recently, Ning and co-workers demonstrated the one-step synthesis of G/SWCNT hybrids by CVD with a mixed catalyst of MgO and Fe/MgO, in which MgO served as the template for the deposition of graphene and Fe/MgO served as the catalyst for the growth of SWCNTs as well as the graphene layers [20]. Besides, with a mixture of NiO and Y_2O_3 , Wu et al. also achieved the one-step synthesis of G/SWCNT hybrids by arc-discharge method, in which the SWCNTs grew from the oversaturated metal carbon liquid alloy and the graphene was formed from the evaporation of graphite under H_2 atmosphere [21]. Therefore, the strategy for the one-step synthesis of G/SWCNT hybrids involved in these reports was more like an *in situ* mixing rather than *in situ* growth process.

The key issue for the *in situ* growth of G/SWCNT hybrids lies in the stability of the catalyst NPs during the deposition of graphene layers. Recently, we reported that layered double hydroxides (LDHs), which are a kind of hydrotalcite-like material composed of positively-charged layers and charge-balancing interlayer anions, exhibited the ability to produce

embedded high density metal NPs with extraordinary thermal stability on the as-calcined layered double oxide (LDO) flakes [22]. SWCNTs with various kinds of architectures were successfully constructed based on the LDH catalyst, including entangled SWCNTs [23], short-aligned SWCNTs [24], and SWCNT double helices [25]. Furthermore, the LDO flakes are mainly composed of metal oxides and spinels, which facilitate the LDO flakes to be used as the template for graphene deposition [26–29]. Therefore, the LDHs are considered as a promising catalyst for the *in situ* growth of G/SWCNT hybrids.

Very recently, we have reported the *in situ* growth of G/SWCNT hybrids with FeMgAl LDH flakes and evaluated their performance as cathode materials for Li–S batteries [30]. In this work, *in situ* deposition of graphene and SWCNTs was carried out by CVD of methane at a high temperature with CoMgAl LDHs as the catalyst precursor. After the removal of CoMgAl LDO flakes, G/SWCNT/ Co_3O_4 hybrids with SWCNTs directly grown on graphene and Co_3O_4 NPs encapsulated in graphene layers were available. CO_2 -oxidation and acid treatment were carried out in sequence to further remove the Co_3O_4 NPs, leading to the formation of G/SWCNT hybrids with high purity. Due to the expected high surface area and enhanced dispersion of graphene and SWCNTs, the G/SWCNT hybrids are considered as promising electrode materials for supercapacitors. The supercapacitors are a kind of highly concerned energy storage devices exhibiting the advantages of high power density, fast recharge capability, and long cycle life [31]. Various kinds of nanostructured carbon materials, such as carbon onions [32–34], nanodiamonds [33], carbide-derived carbons (CDCs) [35–37], CNTs [38,39], graphene [40], and G/CNT hybrids [4,13,21], have been demonstrated good performance for electric double-layer supercapacitors due to their high surface area. For supercapacitors, both the electric double-layer capacitors that require high-SSA carbon materials and pseudocapacitors that require pseudocapacitive materials are highly needed [31]. Herein, the electrochemical performances of the G/SWCNT hybrids with Co_3O_4 NPs for pseudocapacitor and that without Co_3O_4 NPs for double layer capacitor were both evaluated.

2. Experimental

2.1. Catalyst preparation

The CoMgAl LDHs were prepared using a urea assisted coprecipitation reaction. $\text{Mg}(\text{NO}_3)_2 \cdot 6\text{H}_2\text{O}$, $\text{Al}(\text{NO}_3)_3 \cdot 9\text{H}_2\text{O}$, $\text{Co}(\text{NO}_3)_2 \cdot 6\text{H}_2\text{O}$, and urea were dissolved in 250.0 mL deionized water with $[\text{Co}^{2+}] + [\text{Mg}^{2+}] + [\text{Al}^{3+}] = 0.15 \text{ mol/L}$, $n(\text{Co}):n(\text{Mg}):n(\text{Al}) = 0.4:3:1$, $[\text{urea}] = 3.0 \text{ mol/L}$. The solution was kept at 94°C for 12 h without stirring in a flask (equipped with a reflux condenser) of 500.0 mL. CoMgAl LDHs can be obtained after filtering, washing, and freeze-drying of the as-obtained suspension.

2.2. Preparation of the G/SWCNT hybrids

The deposition of graphene and SWCNTs on CoMgAl LDHs were carried out using a high-temperature catalytic CVD. Typically, about 1.0 g CoMgAl LDHs were sprayed uniformly at the center of a horizontal quartz tubular reactor inserted into a

furnace at atmospheric pressure, which was then heated under flowing Ar (600 mL/min). On reaching 950 °C, the flow rate of Ar was turned down to 100 mL/min, and CH₄ (500 mL/min) was then introduced into the reactor for the deposition of graphene and SWCNTs. The reaction was maintained for 15 min at 950 °C before the furnace was cooled down to room temperature under Ar flow.

The as-obtained G/SWCNT/LDO composites were treated by NaOH (12.0 mol/L) aqueous solution at 150 °C for 6 h and HCl (5.0 mol/L) aqueous solution at 80 °C for 3 h, subsequently, to remove the CoMgAl LDO flakes. G/SWCNT/Co₃O₄ hybrids were available after filtering, washing, and freeze-drying. Part of the G/SWCNT/Co₃O₄ hybrids were further treated by a mixture of CO₂ (60 mL/min) and Ar (300 mL/min) at 800 °C in a quartz tube. The as-obtained products were then treated by HCl (5.0 mol/L) aqueous solution again at 80 °C for 3 h to remove the Co₃O₄ NPs. G/SWCNT hybrids with a high carbon purity were available after filtering, washing, and freeze-drying.

2.3. Characterizations

The morphology of the G/SWCNT/LDO, G/SWCNT/Co₃O₄, and G/SWCNT hybrid samples was characterized using a JSM 7401F scanning electron microscope (SEM) operated at 3.0 kV, and a JEM 2010 high resolution transmission electron microscope (TEM) operated at 120.0 kV. The thermogravimetric analysis (TGA) was carried out using TGA/DSC1 STAR^e system under O₂ atmosphere. The Brunauer–Emmett–Teller (BET) SSAs of the samples were measured by N₂ adsorption/desorption at liquid-N₂ temperature using Autosorb-IQ₂-MP-C system. Before measurements, the sample was degassed at 300 °C until a manifold pressure of 2 mmHg was reached. Energy dispersive spectrum (EDS) analysis was performed using a JEM 2010 apparatus equipped with an Oxford Instrument energy dispersive spectrometer with the analytical software INCA, and the acceleration voltage applied was 120.0 kV. Raman spectra were recorded with He–Ne laser excitation at 633 nm using Horiba Jobin Yvon LabRAM HR800 Raman Spectrometer.

All electrochemical measurements were performed in a three-electrode setup, in which Ni foam coated with the G/SWCNT hybrids with or without Co₃O₄ NPs served as the working electrode, a platinum gauze electrode served as the counter electrode, and Hg/HgO electrode served as the reference electrode. The fabrication of working electrodes was carried out as follows: briefly, 95 wt.% of the G/SWCNT hybrids with or without Co₃O₄ NPs and 5 wt.% poly(tetrafluoroethylene) were mixed together with a few drops of ethanol by sonication; The mixture was then pressed onto nickel foam current collectors (1 cm × 1 cm) and dried at 100 °C for 12 h to fabricate the working electrode. The measurements were carried out in a 6.0 mol/L KOH aqueous electrolyte at room temperature using a Solartron 1470E electrochemical station equipped with a 1455A FRA module.

3. Results and discussions

3.1. G/SWCNT/LDO composites

The as-prepared CoMgAl LDHs were well crystallized hexagonal flakes with a lateral size of ca. 1 μm and a thickness of

several nanometers (Fig. 1a and b). Calcination of the CoMgAl LDH flakes led to the transformation to their corresponding CoMgAl LDO flakes with MgO, Co₃O₄ and MgAl₂O₄ as the main components (Fig. 1b). This facilitates the CoMgAl LDO flakes to be effective templates for the deposition of graphene layers at high temperature [26–29]. Reduction of the CoMgAl LDO flakes induces the formation of large quantity of Co NPs with small size embedded on the LDO flakes to catalyze the growth of SWCNTs. Herein, after the CVD of methane on the CoMgAl LDO flakes at a high temperature of 950 °C, the as-obtained products are constituted of SWCNTs interlinked with the flakes (Fig. 1c). TEM image of the products shows the presence of large quantity of catalyst NPs and SWCNTs on the LDO flakes (Fig. 1d). Note that graphene with one or two layers were synchronously deposited on the surface of the CoMgAl LDO flakes (Fig. 1e). Such graphene layers were few detected if the growth temperature was lower than 950 °C [23]. Some of the Co NPs were encapsulated by graphene layers (Fig. 1e). Fig. 1f shows the growth of a SWCNT from a catalyst NP, in which extra graphene layers can be observed outside the catalyst NPs in addition to the SWCNT, as indicated by the arrow. This can be attributed to the deposition of graphene layers around the catalyst NPs, and is a significant difference with the situation that only SWCNTs were deposited on LDO flakes [41], indicating that the Co NPs facilitate the connection between the graphene layers and SWCNTs during the *in situ* CVD.

3.2. G/SWCNT/Co₃O₄ hybrids

The CoMgAl LDO flakes were removed by subsequent alkali and acid treatments. The as-obtained products, which were composed of SWCNTs grown on the surface of graphene layers with large quantity of NPs, presented similar morphology with the G/SWCNT/LDO hybrids (Fig. 2a–c). Fig. 2d shows the morphology of the connection between SWCNTs and graphene layers, and extra graphene layers at the connected interface were also detected after the removal of the catalyst NPs. Graphene with similar size to the original CoMgAl LDO flakes were detected to be with few layers, as is shown in Fig. 2b–d. Some NPs were not fully removed by the simple purification treatment because of the entire encapsulation of graphene layers (Fig. 2d). They were demonstrated to be Co₃O₄ NPs by the high resolution TEM image (Fig. 2e), which were originated from Co NPs attributed to the oxidation in air or during the purification. The Co₃O₄ NPs were with a small and uniform size distribution concentrated in the range of 4–6 nm (Fig. 2f). The strong radial breathing mode (RBM) peaks shown in the Raman spectra between 100 and 300 cm⁻¹ indicated the existence of SWCNTs in the G/SWCNT/Co₃O₄ hybrids (Fig. 2g). The I_D/I_G ratio showed a high value of 0.52, which is possibly resulted from the existence of large amount of Co₃O₄@C NPs composed of Co₃O₄ NPs encapsulated by graphene layers. The intrinsic peaks observed around 469 and 673 cm⁻¹ in the Raman spectra further demonstrated the presence of large amount of Co₃O₄ [42]. The TGA curve shown in Fig. 2h indicated that the mass ratio of Co₃O₄ in the G/SWCNT/Co₃O₄ hybrids was around 27.3 wt.%. The EDS analysis showed that other elements in the CoMgAl LDOs, such as Mg and Al, have been completely

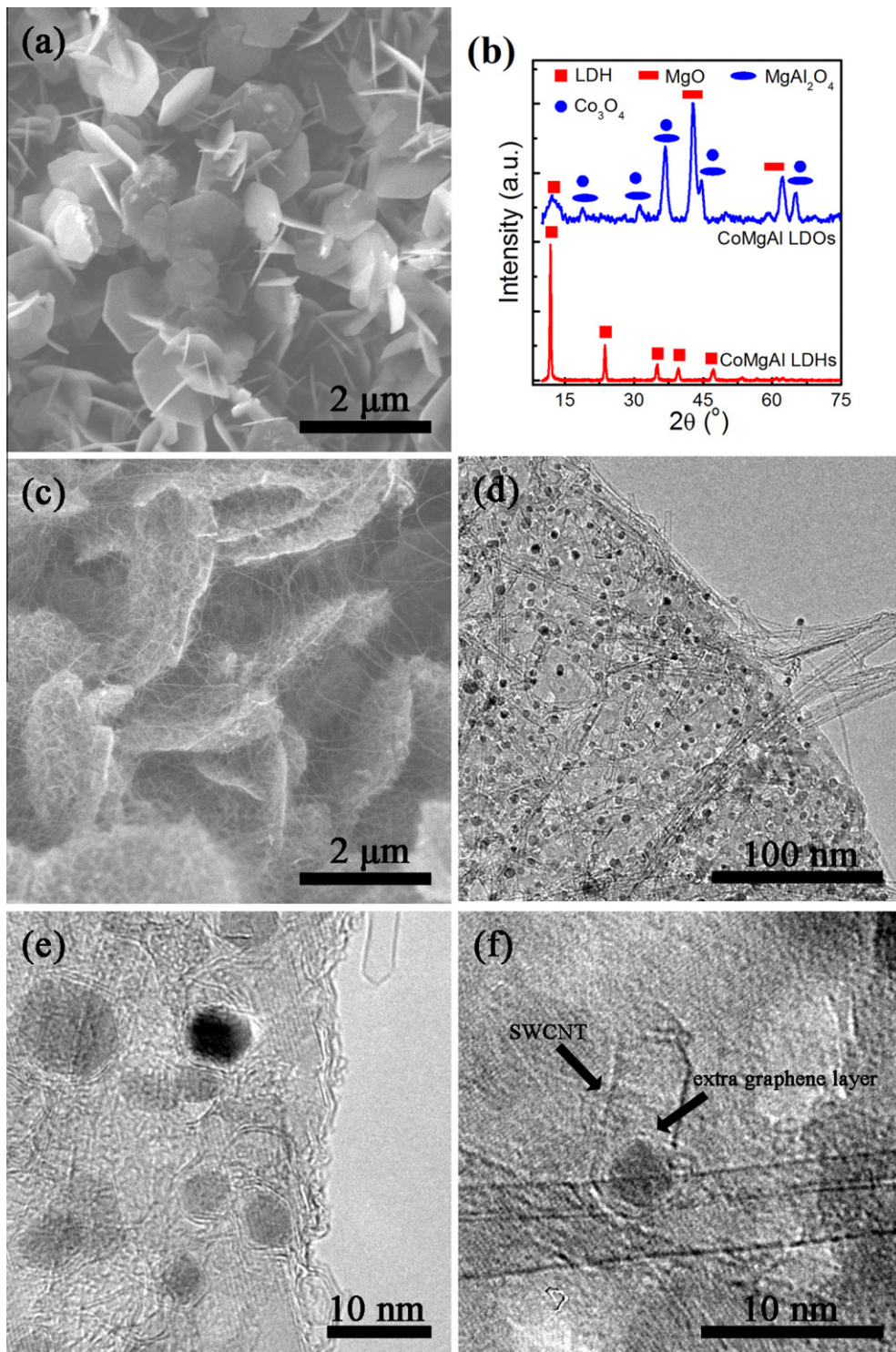


Fig. 1 – (a) SEM image of the CoMgAl LDH flakes; (b) XRD patterns of the CoMgAl LDHs and the corresponding CoMgAl LDOs; (c) SEM, (d) TEM, and (e, f) high resolution TEM images of the as-grown G/SWCNT/LDO composites from CoMgAl LDH flakes.

removed. Therefore, a kind of G/SWCNT/Co₃O₄ hybrid was available.

3.3. G/SWCNT hybrids

To obtain the G/SWCNT hybrids with a high carbon purity, the Co₃O₄@C NPs as shown in Fig. 3a should be removed by

further purification. Herein, a CO₂-oxidation strategy was proposed to open the graphene shell and provide the acid channel. When the temperature was higher than 700 °C, CO₂ reacted with solid carbon through reproporation and generated CO [43,44]:



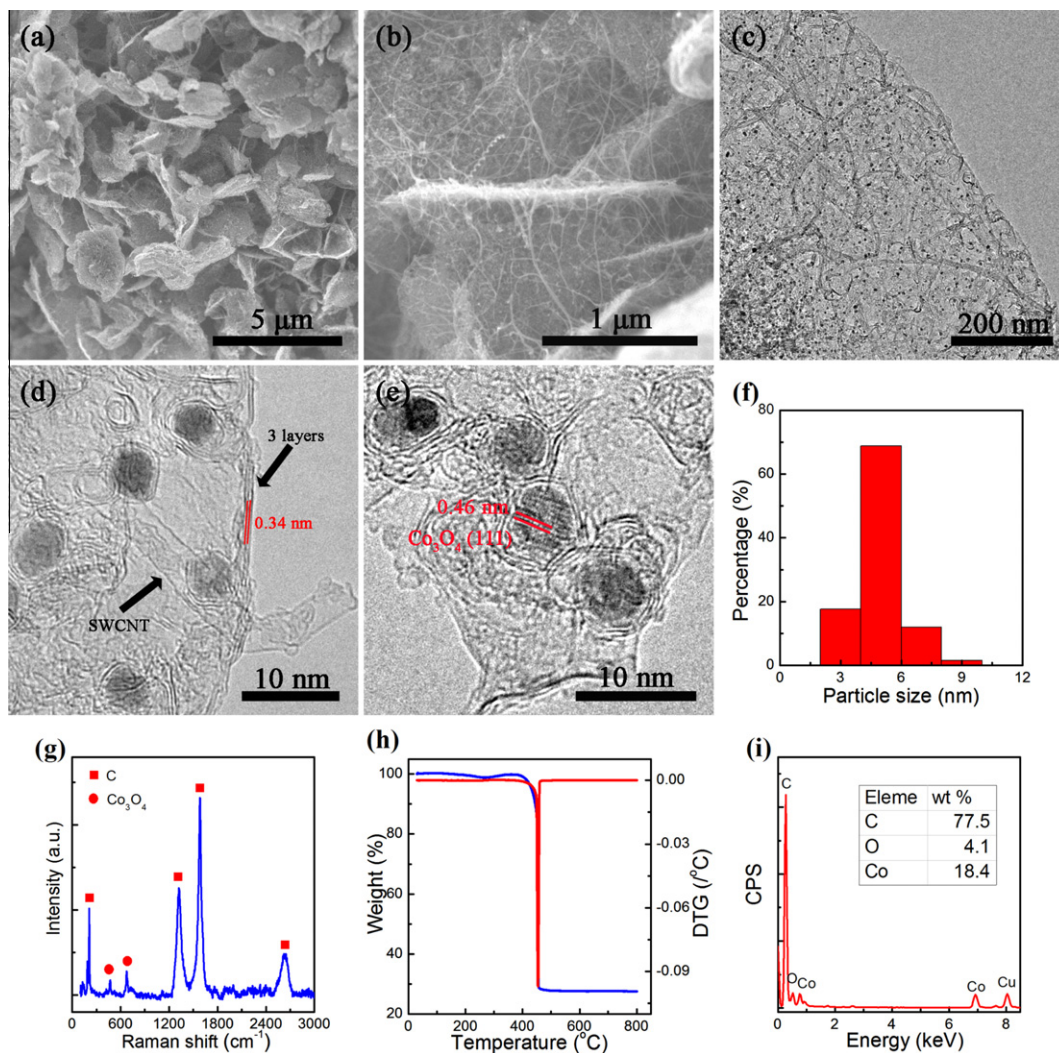


Fig. 2 – (a, b) SEM and (c) TEM images of the G/SWCNT/Co₃O₄ hybrids; (d, e) high resolution TEM images of the G/SWCNT/Co₃O₄ hybrids; (f) particle size distribution of the Co₃O₄ NPs in the G/SWCNT/Co₃O₄ hybrids; (g) Raman spectrum, (h) TGA, and (i) EDS profiles of the G/SWCNT/Co₃O₄ hybrids.

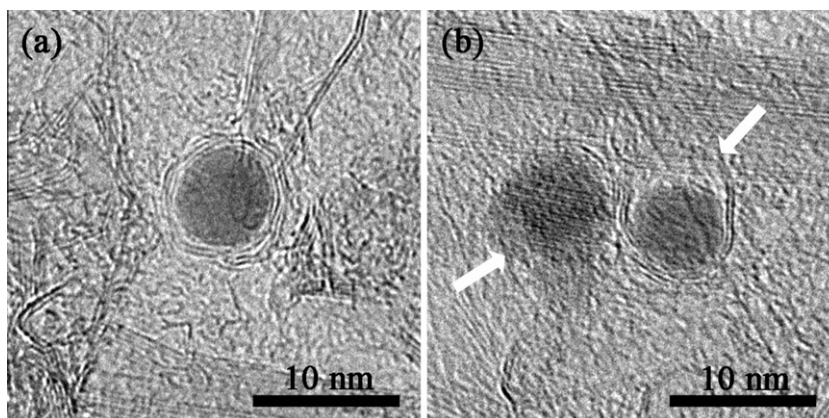


Fig. 3 – High resolution TEM images of the Co₃O₄@NPs (a) before and (b) after the CO₂-oxidation treatment.

A surface oxygen complex (C(O)) was initially formed and subsequently became stable under the reaction conditions, acting as a retardant by blocking the reaction sites:



It may also decompose and leave the surface as CO



Meanwhile, the metal oxide particle will be reduced into carbon, as shown by



The as-obtained Co NPs have a high density of electrons. As a result, the CO_2 was more readily to attack carbon-catalyst interface, and the Co NPs can serve as catalyst for Reaction (1). Therefore, the encapsulating graphene can be selectively etched. This is confirmed by the high resolution TEM images, as shown in Fig. 3b. Parts of the graphene layers that encapsulated around the Co_3O_4 NPs were effectively etched away after treated by CO_2 at 800°C for 30 min, and thus provided the channels for the diffusion of acid molecular to metal-containing NPs.

Fig. 4a and b shows the TEM images of the products obtained after the CO_2 -oxidation treatment and acid washing. The Co_3O_4 NPs have been effectively removed by the acid treatment, but few damages occurred on the graphene layers

and the SWCNTs. TGA curve shown in Fig. 4c indicates that the as-obtained G/SWCNT hybrids exhibited a high carbon purity of 98.4 wt.%. After the CO_2 -oxidation treatment, no obvious difference was observed on the Raman spectra but the value of the I_D/I_G ratio reduced to 0.25. The intrinsic peaks corresponding to the existence of Co_3O_4 can still be observed with a small shift to 463 and 667 cm^{-1} , indicating the partial reduction of the Co_3O_4 to Co. However, these peaks completely disappeared after the followed acid treatment and the I_D/I_G ratio for the final G/SWCNT hybrids was further reduced to 0.06. Therefore, the CO_2 -oxidation assistant purification was effective for the removal of encapsulated Co_3O_4 NPs from the G/SWCNT/ Co_3O_4 hybrids.

Comparison of the characteristics of the G/SWCNT/ Co_3O_4 and G/SWCNT hybrids was shown in Table 1. The mass ratio of Co_3O_4 was reduced from 27.3 wt.% for the G/SWCNT/ Co_3O_4 hybrids to 1.6 wt.% for the G/SWCNT hybrids, along with the improvement of their thermal stability. The removal of Co_3O_4 NPs led to a significant increase of SSA of the hybrids from $451.8\text{ m}^2/\text{g}$ to $807.0\text{ m}^2/\text{g}$. The total pore volume of the hybrids was also increased from $1.21\text{ cm}^3/\text{g}$ to $2.33\text{ cm}^3/\text{g}$. In spite of the significant reduction of the I_D/I_G ratio, the position of 2D peaks for the hybrids was also reduced from 2623.1 cm^{-1} to 2609.3 cm^{-1} , indicating the existence of large amount of single-layered graphene and SWCNTs [28,45].

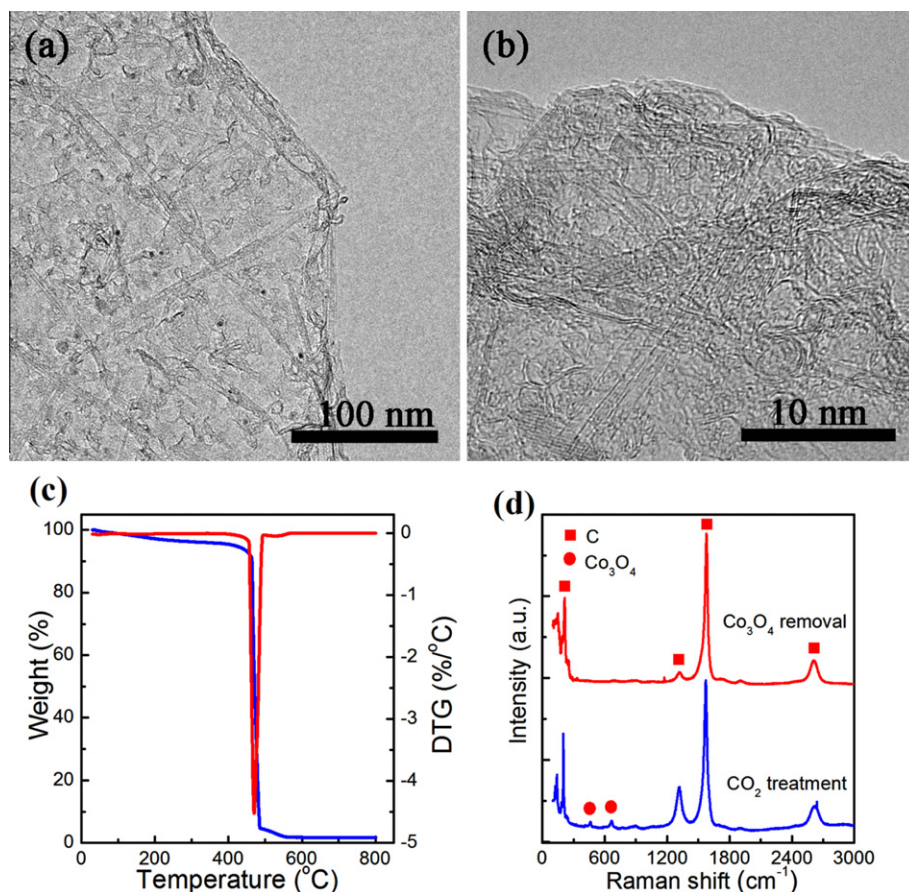


Fig. 4 – (a, b) TEM images and (c) TGA result of the G/SWCNT hybrids after the removal of Co_3O_4 NPs; (d) Raman spectra of the G/SWCNT hybrids after the CO_2 -oxidation treatment and the removal of Co_3O_4 NPs.

Table 1 – Comparison of the characteristics of the G/SWCNT/Co₃O₄ and G/SWCNT hybrids.

Hybrid samples	Co ₃ O ₄ content (wt.%)	Weight loss peak (°C)	SSA (m ² /g)	Pore volume (cm ³ /g)	I _D /I _G	2D (cm ⁻¹)
G/SWCNT/Co ₃ O ₄	27.3	453.3	451.8	1.21	0.52	2623.1
G/SWCNT	1.6	470.0	807.0	2.33	0.06	2609.3

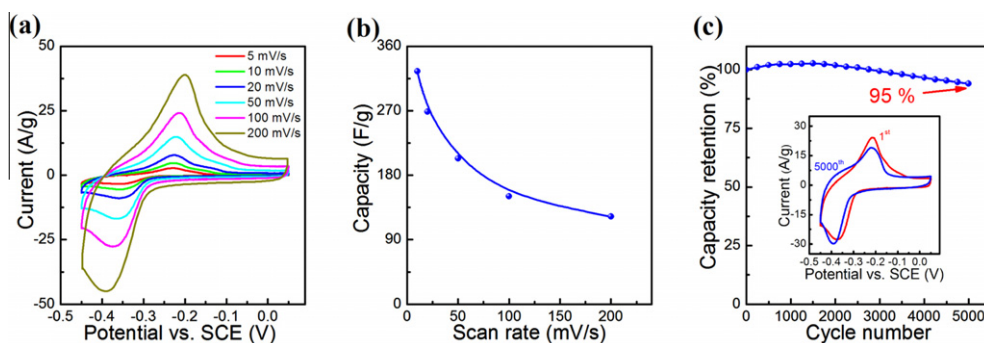


Fig. 5 – Electrochemical performance of the G/SWCNT/Co₃O₄ hybrids as electrode materials for pseudo-capacitors in 6 M KOH solution: (a) CV curves at different scan rates; (b) capacity at different scan rates; (c) cyclic performance. The inserted figure in (c) is the comparison of the CV curves for the first and 5000th cycles.

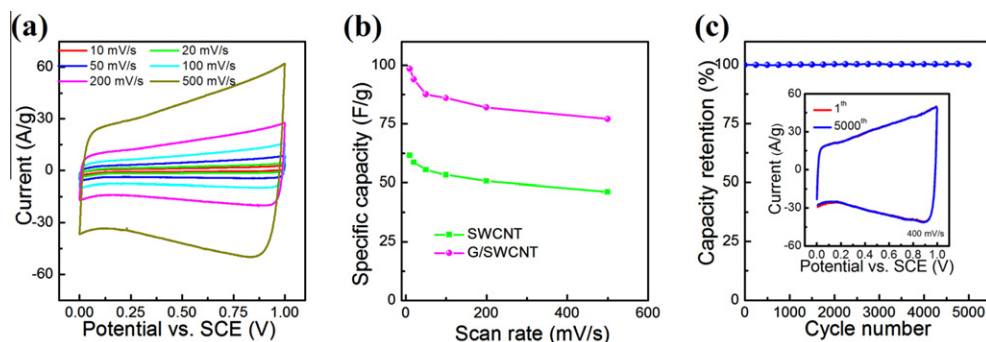
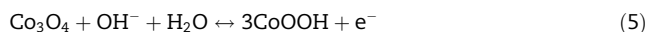


Fig. 6 – Electrochemical performance of the G/SWCNT hybrids as electrode materials for double-layer capacitors in 6 M KOH solution: (a) CV curves at different scan rates; (b) capacity at different scan rates with the comparison of SWCNTs; (c) cyclic performance. The inserted figure in (c) is the comparison of the CV curves for the first and 5000th cycles.

3.4. Electrochemical evaluation

Attributed from the low environmental footprint, excellent redox activity, and extremely high theoretical pseudocapacity of ca. 3560 F/g, Co₃O₄ was widely explored for pseudocapacitors. How to fabricate a conductive network to fully demonstrate the potential of such Co₃O₄ materials is a great challenge. Herein, the G/SWCNT/Co₃O₄ hybrids are expected to be a promising electrode candidate to demonstrate the pseudocapacitance of Co₃O₄. Fig. 5a shows the cyclic voltammetry (CV) curves measured in the potential window from –0.45 to 0.05 V. The sharp oxidation peak at –0.25 V in the anodic scan and the prominent reduction peak at –0.33 V in the cathodic scan are a result of the following redox reaction [46,47]:



With the increase of the scan rate, significant increases of the current were detected. At a scan rate of 10 mV/s, a high capacitance of 325 F/g_{electrode} was obtained, which reduced

to 122 F/g_{electrode} at a scan rate of 200 mV/s (Fig. 5b). The cyclic stability of the G/SWCNT/Co₃O₄ hybrids at a scan rate of 100 mV/s for 5000 cycles is shown in Fig. 5c, in which the CV curves for the 1st and 5000th cycles were inserted. During the first 2000 cycles, a small increase of the capacity occurred due to the increased effective interfacial area between the cobalt hydroxide and electrolyte with the increase of reaction time. After 5000 cycles, 95% of the capacity was retained, indicating the electrochemical stability of the G/SWCNT/Co₃O₄ hybrids electrode material was acceptable.

Pure carbon materials with high SSA are considered as one of the best electrode materials for the double-layer capacitors with excellent stability. Here, the SSA of the as-purified G/SWCNT hybrids (807.0 m²/g) is a little higher than that of SWCNTs (756.8 m²/g) with similar purity prepared with the same CoMgAl LDHs at a lower growth temperature of 900 °C [23]. Electrochemical performance of the G/SWCNT hybrids was evaluated with the comparison of SWCNTs in KOH aqueous solution. The CV curves for the G/SWCNT hybrid elec-

trode measured in the potential window from 0 to 1.0 V are shown in Fig. 6a. All the CV curves at different scan rates ranging from 10 to 500 mV/s show the rectangular shape without obvious redox peaks, indicating an ideal double-layer capacitive behavior. As shown in Fig. 6b, a high capacity of 98.5 F/g_{electrode} was available at a scan rate of 10 mV/s, which reduced to 77.0 F/g_{electrode} when the scan rate increased to 500 mV/s, indicating that 78.2% of the capacity was retained. For comparison, the capacities for the G/SWCNTs at different scan rates were all much larger than that of SWCNTs. The capacity for the SWCNT electrode material at a scan rate of 10 mV/s was 61.6 F/g_{electrode}, which reduced to 46.2 F/g_{electrode} when the scan rate increased to 500 mV/s with a 75.0% retention. The capacitance of the G/SWCNT hybrids might still be limited when compared with carbon nanomaterials that with much higher surface area, such as CDCs [35,37] and activated graphene [48]. However, an improvement of ca. 60% has been achieved when compared with SWCNTs even though they were with similar SSA. This indicates that the combination of graphene and SWCNTs into G/SWCNT hybrids to enhance the dispersion of SWCNTs is an effective route to improve their electrochemical performance. Fig. 6c shows the cyclic performance of the G/SWCNT hybrid electrode material. No capacity decay and shape change of the CV curve can be observed even after 5000 cycles, indicating the G/SWCNT hybrids were with extraordinary structure stability for the double-layer capacitors.

4. Conclusions

In situ growth of graphene and SWCNTs was successfully achieved by CVD of methane at a high temperature of 950 °C with CoMgAl LDHs as the catalyst precursor. Removal of the CoMgAl LDO flakes led to the formation of G/SWCNT/Co₃O₄ hybrids with the morphology of SWCNTs interlinked with graphene layers. The Co₃O₄ NPs, which were encapsulated in graphene layers in the G/SWCNT/Co₃O₄ hybrids, were with a high concentration of 27.3 wt.% and a uniform size distribution concentrated in 4–6 nm. G/SWCNT hybrids with a high carbon purity and high SSA can be obtained by the removal of the Co₃O₄ NPs through a CO₂-oxidation assistant purification method. Both the G/SWCNT/Co₃O₄ and G/SWCNT hybrids showed good electrochemical performance for supercapacitors. The G/SWCNT/Co₃O₄ hybrids can serve as promising electrode materials for pseudo-capacitors with a high capacity of 325 F/g_{electrode}. In another aspect, the G/SWCNT hybrids can be used as good electrode materials for double-layer capacitors with high capacity, good rate and cyclic performances. The fabrication of the G/SWCNT/Co₃O₄ and G/SWCNT hybrids is easy to be scaled up for their further applications in the area of composites, energy storage, catalysis, and devices.

Acknowledgements

The author thanks Dr. Chao Zheng and Mr. Yuntao Yu for helpful discussion. This work was supported by National Basic Research Program of China (973 Program, 2011CB932602) and Beijing City Innovative Scientific Program (20121097711).

REFERENCES

- [1] Xu L, Wei N, Zheng Y, Fan Z, Wang H-Q, Zheng J-C. Graphene-nanotube 3D networks: intriguing thermal and mechanical properties. *J Mater Chem* 2011;22(4):1435–44.
- [2] Cai D, Song M, Xu C. Highly conductive carbon-nanotube/graphite-oxide hybrid films. *Adv Mater* 2008;20(9):1706–9.
- [3] Tung VC, Chen LM, Allen MJ, Wassei JK, Nelson K, Kaner RB, et al. Low-temperature solution processing of graphene-carbon nanotube hybrid materials for high-performance transparent conductors. *Nano Lett* 2009;9(5):1949–55.
- [4] Wang Y, Wu Y, Huang Y, Zhang F, Yang X, Ma Y, et al. Preventing graphene sheets from restacking for high-capacitance performance. *J Phys Chem C* 2011;115(46):23192–7.
- [5] Bon SB, Valentini L, Kenny JM, Peponi L, Verdejo R, Lopez-Manchado MA. Electrodeposition of transparent and conducting graphene/carbon nanotube thin films. *Phys Status Solidi A* 2010;207(11):2461–6.
- [6] Hong T-K, Lee DW, Choi HJ, Shin HS, Kim B-S. Transparent, flexible conducting hybrid multi layer thin films of multiwalled carbon nanotubes with graphene nanosheets. *ACS Nano* 2010;4(7):3861–8.
- [7] Byon HR, Lee SW, Chen S, Hammond PT, Shao-Horn Y. Thin films of carbon nanotubes and chemically reduced graphenes for electrochemical micro-capacitors. *Carbon* 2011;49(2):457–67.
- [8] Shao JJ, Lv W, Guo QG, Zhang C, Xu Q, Yang QH, et al. Hybridization of graphene oxide and carbon nanotubes at the liquid/air interface. *Chem Commun* 2012;48(31):3706–8.
- [9] Chen S, Chen P, Wang Y. Carbon nanotubes grown *in situ* on graphene nanosheets as superior anodes for Li-ion batteries. *Nanoscale* 2011;3(10):4323–9.
- [10] Paul RK, Ghazinejad M, Penchev M, Lin J, Ozkan M, Ozkan CS. Synthesis of a pillared graphene nanostructure: a counterpart of three-dimensional carbon architectures. *Small* 2010;6(20):2309–13.
- [11] Lv RT, Cui TX, Jun MS, Zhang Q, Cao AY, Su DS, et al. Open-ended, N-doped carbon nanotube-graphene hybrid nanostructures as high-performance catalyst support. *Adv Funct Mater* 2011;21(5):999–1006.
- [12] Yu KH, Lu GH, Bo Z, Mao S, Chen JH. Carbon nanotube with chemically bonded graphene leaves for electronic and optoelectronic applications. *J Phys Chem Lett* 2011;2(13):1556–62.
- [13] Fan ZJ, Yan J, Zhi L, Zhang Q, Wei T, Feng J, et al. A three-dimensional carbon nanotube/graphene sandwich and its application as electrode in supercapacitors. *Adv Mater* 2010;22(33):3723–8.
- [14] Fan ZJ, Yan J, Wei T, Ning GQ, Zhi LJ, Liu JC, et al. Nanographene-constructed carbon nanofibers grown on graphene sheets by chemical vapor deposition: high-performance anode materials for lithium ion batteries. *ACS Nano* 2011;5(4):2787–94.
- [15] Zhang LL, Xiong Z, Zhao XS. Pillaring chemically exfoliated graphene oxide with carbon nanotubes for photocatalytic degradation of dyes under visible light irradiation. *ACS Nano* 2010;4(11):7030–6.
- [16] Li S, Luo Y, Lv W, Yu W, Wu S, Hou P, et al. Vertically aligned carbon nanotubes grown on graphene paper as electrodes in lithium-ion batteries and dye-sensitized solar cells. *Adv Energy Mater* 2011;1(4):486–90.
- [17] Du F, Yu D, Dai L, Ganguli S, Varshney V, Roy AK. Preparation of tunable 3D pillared carbon nanotube-graphene networks for high-performance capacitance. *Chem Mater* 2011;23(21):4810–6.

- [18] Rinaldi A, Tessonnier J-P, Schuster ME, Blume R, Girgsdies F, Zhang Q, et al. Dissolved carbon controls the initial stages of nanocarbon growth. *Angew Chem Int Ed* 2011;50(14):3313–3317.
- [19] Lee DH, Kim JE, Han TH, Hwang JW, Jeon S, Choi SY, et al. Versatile carbon hybrid films composed of vertical carbon nanotubes grown on mechanically compliant graphene films. *Adv Mater* 2010;22(11):1247–52.
- [20] Zhu X, Ning G, Fan Z, Gao J, Xu C, Qian W, et al. One-step synthesis of a graphene-carbon nanotube hybrid decorated by magnetic nanoparticles. *Carbon* 2012;50(8):2764–71.
- [21] Wu YP, Zhang TF, Zhang F, Wang Y, Ma YF, Huang Y, et al. In situ synthesis of graphene/single-walled carbon nanotube hybrid material by arc-discharge and its application in supercapacitors. *Nano Energy* 2012;1(6):820–7.
- [22] Zhao M-Q, Zhang Q, Zhang W, Huang J-Q, Zhang Y, Su DS, et al. Embedded high density metal nanoparticles with extraordinary thermal stability derived from guest-host mediated layered double hydroxides. *J Am Chem Soc* 2010;132(42):14739–41.
- [23] Zhao M-Q, Zhang Q, Huang J-Q, Nie J-Q, Wei F. Layered double hydroxides as catalysts for the efficient growth of high quality single-walled carbon nanotubes in a fluidized bed reactor. *Carbon* 2010;48(11):3260–70.
- [24] Zhao M-Q, Tian G-L, Zhang Q, Huang J-Q, Nie J-Q, Wei F. Preferential growth of short aligned, metallic-rich single-walled carbon nanotubes from perpendicular layered double hydroxide film. *Nanoscale* 2012;4(7):2470–7.
- [25] Zhao M-Q, Zhang Q, Tian G-L, Huang J-Q, Wei F. Space confinement and rotation stress induced self-organization of double-helix nanostructure: a nanotube twist with a moving catalyst head. *ACS Nano* 2012;6(5):4520–9.
- [26] Ruemmel MH, Bachmatiuk A, Scott A, Boerrnert F, Warner JH, Hoffman V, et al. Direct low-temperature nanographene CVD synthesis over a dielectric insulator. *ACS Nano* 2010;4(7):4206–10.
- [27] Xie K, Qin X, Wang X, Wang Y, Tao H, Wu Q, et al. Carbon nanocages as supercapacitor electrode materials. *Adv Mater* 2012;24(3):347–52.
- [28] Ning G, Fan Z, Wang G, Gao J, Qian W, Wei F. Gram-scale synthesis of nanomesh graphene with high surface area and its application in supercapacitor electrodes. *Chem Commun* 2011;47(21):5976–8.
- [29] Ruemmel MH, Kramberger C, Grueneis A, Ayala P, Gemming T, Buechner B, et al. On the graphitization nature of oxides for the formation of carbon nanostructures. *Chem Mater* 2007;19(17):4105–7.
- [30] Zhao MQ, Liu XF, Zhang Q, Tian GL, Huang JQ, Zhu WC, et al. Graphene/single-walled carbon nanotube hybrids: one-step catalytic growth and applications for high-rate Li-S batteries. *ACS Nano* 2012. <http://dx.doi.org/10.1021/nn304037d>.
- [31] Simon P, Gogotsi Y. Materials for electrochemical capacitors. *Nat Mater* 2008;7(11):845–54.
- [32] McDonough JK, Frollov AI, Presser V, Niu J, Miller CH, Ubierto T, et al. Influence of the structure of carbon onions on their electrochemical performance in supercapacitor electrodes. *Carbon* 2012;50(9):3298–309.
- [33] Portet C, Yushin G, Gogotsi Y. Electrochemical performance of carbon onions, nanodiamonds, carbon black and multiwalled nanotubes in electrical double layer capacitors. *Carbon* 2007;45(13):2511–8.
- [34] Borgohain R, Li J, Selegue JP, Cheng YT. Electrochemical study of functionalized carbon nano-onions for high-performance supercapacitor electrodes. *J Phys Chem C* 2012;116(28):15068–75.
- [35] Presser V, Zhang L, Niu JJ, McDonough J, Perez C, Fong H, et al. Flexible nano-felts of carbide-derived carbon with ultra-high power handling capability. *Adv Energy Mater* 2011;1(3):423–30.
- [36] Gao Y, Presser V, Zhang L, Niu JJ, McDonough JK, Perez CR, et al. High power supercapacitor electrodes based on flexible TiC-CDC nano-felts. *J Power Sources* 2012;201:368–75.
- [37] Rose M, Korenblit Y, Kockrick E, Borchardt L, Oschatz M, Kaskel S, et al. Hierarchical micro- and mesoporous carbide-derived carbon as a high-performance electrode material in supercapacitors. *Small* 2011;7(8):1108–17.
- [38] Simon P, Gogotsi Y. Capacitive energy storage in nanostructured carbon-electrolyte systems. *Acc Chem Res* 2012. <http://dx.doi.org/10.1021/ar200306b>.
- [39] Xu GH, Zheng C, Zhang Q, Huang JQ, Zhao MQ, Nie JQ, et al. Binder-free activated carbon/carbon nanotube paper electrodes for use in supercapacitors. *Nano Res* 2011;4(9):870–81.
- [40] Zhang LL, Zhou R, Zhao XS. Graphene-based materials as supercapacitor electrodes. *J Mater Chem* 2010;20(29):5983–92.
- [41] Zhao MQ, Zhang Q, Jia XL, Huang JQ, Zhang Y-H, Wei F. Hierarchical composites of single/double-walled carbon nanotubes interlinked flakes from direct carbon deposition on layered double hydroxides. *Adv Funct Mater* 2010;20(4):677–85.
- [42] Kovanda F, Rojka T, Dobesova J, Machovic V, Bezdicka P, Obalova L, et al. Mixed oxides obtained from Co and Mn containing layered double hydroxides: preparation, characterization, and catalytic properties. *J Solid State Chem* 2006;179(3):812–23.
- [43] Marsh H, Rodriguez-Reinoso F. Activated carbon. Amsterdam: Elsevier; 2006. p. 243–321.
- [44] Huang JQ, Zhang Q, Zhao MQ, Wei F. The release of free standing vertically-aligned carbon nanotube arrays from a substrate using CO₂ oxidation. *Carbon* 2010;48(5):1441–50.
- [45] Ferrari AC, Meyer JC, Scardaci V, Casiraghi C, Lazzeri M, Mauri F, et al. Raman spectrum of graphene and graphene layers. *Phys Rev Lett* 2006;97(18):187401–1–4.
- [46] Xu J, Gao L, Cao J, Wang W, Chen Z. Preparation and electrochemical capacitance of cobalt oxide (Co₃O₄) nanotubes as supercapacitor material. *Electrochim Acta* 2010;56(2):732–6.
- [47] Zhou W, Liu J, Chen T, Tan KS, Jia X, Luo Z, et al. Fabrication of Co₃O₄-reduced graphene oxide scrolls for high-performance supercapacitor electrodes. *Phys Chem Chem Phys* 2011;13(32):14462–5.
- [48] Zhu Y, Murali S, Stoller MD, Ganesh KJ, Cai W, Ferreira PJ, et al. Carbon-based supercapacitors produced by activation of graphene. *Science* 2011;332(6037):1537–41.